Ammonium Bisulfate/Water Equilibrium and Metastability Phase Diagrams

Dan G. Imre,*,† Jun Xu,‡ I. N. Tang,† and R. McGraw†

Environmental Chemistry Division, Department of Applied Science, Brookhaven National Laboratory, Upton, New York 11973 and Institute of Terrestrial and Planetary Atmospheres, State University of New York, New York 11794

Received: February 5, 1997; In Final Form: March 31, 1997[⊗]

Though ammonium bisulfate is one of the most common of atmospheric hygroscopic aerosols, knowledge of its interaction with water has, until now, been extremely limited. This paper presents our observations on single isolated ammonium bisulfate aerosol particles, as they interact with water vapor at temperatures ranging from −40 to 30 °C. The complete phase diagram in the temperature/composition as well as the pressure/temperature domains has been derived here for the first time, mapping out equilibrium and metastable to stable phase transitions. A new low-temperature crystalline hydrate phase that might have an important role in processes occurring in the upper troposphere has been discovered.

Introduction

Hygroscopic aerosols, both natural and anthropogenic, are ubiquitous in the atmosphere. They serve as cloud condensation nuclei, redistribute atmospheric radiation, and provide sites for condensed phase reactions. These aerosols influence the climate either directly by scattering solar radiation back to space or indirectly by changing the optical properties and frequency of clouds.[1]

Sulfates, which have both natural and anthropogenic sources, are one of the most important atmospheric aerosols. They originate from sulfuric acid molecules which are produced by gas phase photochemical processes. These acidic aerosols are neutralized very rapidly in the lower atmosphere by reactions with ammonia. At low altitudes, therefore, where ammonia concentrations are high, the most common aerosol forms are $(NH_4)_2SO_4$ and $(NH_4)_3H(SO_4)_2$,[2] while above the boundary layer the composition is closer to NH_4HSO_4. Under strong convective conditions NH_4HSO_4 aerosols can also be found at cirrus cloud altitudes where they could serve as ice-forming nuclei (IFN).

We present in this article, a brief summary of our observations on single suspended NH_4HSO_4 particles and their interaction with water vapor, at temperatures ranging from −40 to 30 °C. We have generated the NH_4HSO_4/H_2O phase diagram, and discovered a new crystalline hydrate phase that is stable at temperatures below −30 °C. We have been able to map out deliquescence, efflorescence, and solid-solid phase transitions and show that, unlike most hygroscopic aerosols, NH_4HSO_4 exhibits a strong temperature-dependent deliquescence behavior.

Experimental Section

The single particle levitation technique which was used for these studies has been described in detail elsewhere. It is essentially a low-temperature version of the one used in earlier studies.[3,4] A single electrostatically charged 5 −10 μm (diameter) NH_4HSO_4/H_2O droplet is suspended in an electrodynamic balance. First, the NH_4HSO_4 droplet is dried under vacuum at ∼260 K. Once dry, the particle is balanced in a dc field, and the voltage required to position the particle at the null point is noted. Water vapor is introduced gradually, and the pressure is monitored continuously using a capacitance manometer. The change in the particle's composition as the temperature or relative humidity (RH) is varied is determined by measuring the mass-to-charge ratio (with an accuracy of ∼1%).

A vertically polarized HeNe laser is focused on the particle. The intensity of the scattered light is continuously monitored at a 90° angle from the incident laser, and the phase (solid or liquid) is determined from the Mie scattering.

To assure uniform temperature, the electrodynamic trap and the interaction chamber are constructed of copper. The chamber is insulated with a vacuum shroud and is in contact with a liquid nitrogen reservoir via heat transfer straps. An automated feedback heating loop is used to control the temperature to better than 0.2 K. The temperature is monitored at two points, above and below the particle, with the difference kept to less than 0.3 K. The reported temperature is the average between the two points. The system can be used to perform experiments at constant temperature or to scan temperature at a prescribed rate. Both modes were utilized to obtain the data presented here. When the temperature was scanned, the water vapor pressure was maintained at equilibrium with ice, by coating the cell walls with ice. The entire pressure and temperature monitoring system was calibrated against the ice frost line. The results reported here represent observations of over ∼20 particles.

Experimental Results

Figure 1 illustrates a hydration and dehydration cycle in a plot of particle mass expressed as the mole ratio H_2O/NH_4HSO_4 vs RH. (The RH throughout this paper is always calculated with respect to liquid water according to Tabata.[5]) The cycle in Figure 1 is typical and, qualitatively, is much like the one observed at 25 °C,[6] except that it was carried out at −25 °C. The path A to B represents the anhydrous NH_4HSO_4; at point B, the deliquescence point at −25 °C, the particle absorbs water rapidly to form the saturated NH_4HSO_4 solution droplet at point C. Based on the particle mass, the saturated solution concentration at −25 °C is 41% NH_4HSO_4 by mass. At this temperature the deliquescence point is at 58% RH compared to 40% RH at 25 °C.[6,7] Increasing the RH beyond the deliquescence point produces a more dilute solution droplet at point D. The dehydration path (D−E) shows typical hysteresis, with the range C to E representing the metastable supersaturated solution. At this temperature efflorescence (point E) occurs at 34% RH.

* To whom correspondence should be addressed.
† Brookhaven National Laboratory.
‡ State University of New York.
⊗ Abstract published in *Advance ACS Abstracts,* May 15, 1997.

S1089-5639(97)00442-8 CCC: $14.00

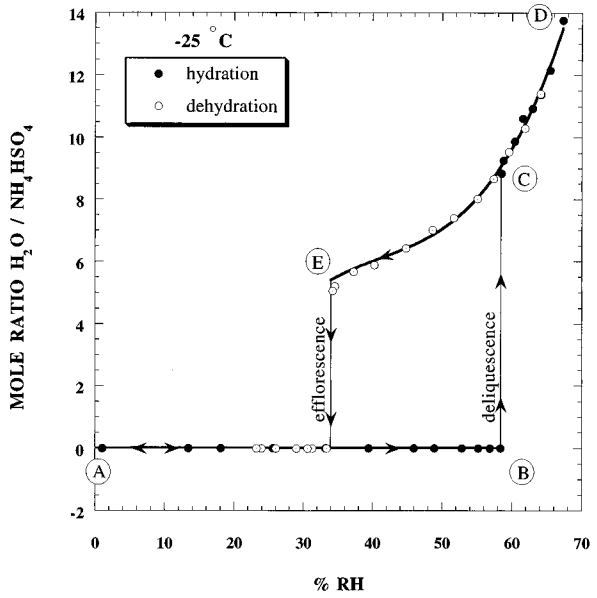

Figure 1. A hydration (A−B−C−D)/dehydration (D−E−A) cycle at −25 °C presented in a plot of particle mass expressed in mole ratio H_2O/NH_4HSO_4 vs %RH. The anhydrous phase deliquesces at 58% RH (B−C), and the supersaturated solution effloresces during the reverse path at 34% RH (E).

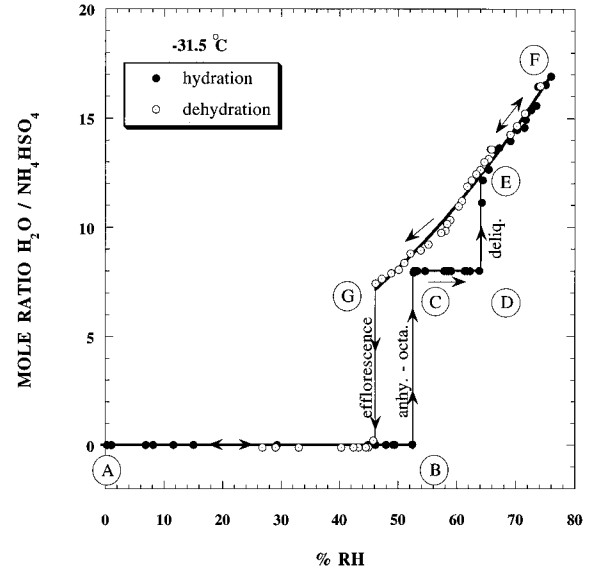

Figure 2. A hydration (A−B−C−D−E−F)/dehydration (F−G−A) cycle at −31.5 °C presented in a plot of particle mass expressed in mole ratio H_2O/NH_4HSO_4 vs % RH. At this temperature the path of increasing RH induces a transition at 52.5% RH (B−C) from the anhydrous phase to $NH_4HSO_4 \cdot 8H_2O$, which is the stable phase at this temperature from 52.5% RH to 64% RH (C−D). The deliquescence point of the octahydrate phase (D−E) is at 64% RH. On the dehydration path the supersaturated solution effloresces at an RH lower than the anhydrous to octahydrate phase transition (G). Consequently, on the dehydration path the octahydrate phase does not form at this temperature.

A similar hydration and dehydration cycle carried out at −31.5 °C is shown in Figure 2. The path A to B is the anhydrous NH_4HSO_4. At 52.5% RH a new feature appears where the solid particle absorbs exactly eight water molecules per molecule of NH_4HSO_4 (B−C) to form a new solid of composition NH_4HSO_4 octahydrate ($NH_4HSO_4 \cdot 8H_2O$). The stable phase between 52.5% RH and 64% RH (C−D) is $NH_4HSO_4 \cdot 8H_2O$. At 64% RH, $NH_4HSO_4 \cdot 8H_2O$ deliquesces to form the 34% NH_4HSO_4 (by mass) solution droplet (E), the concentration of a saturated, with respect to $NH_4HSO_4 \cdot 8H_2O$,

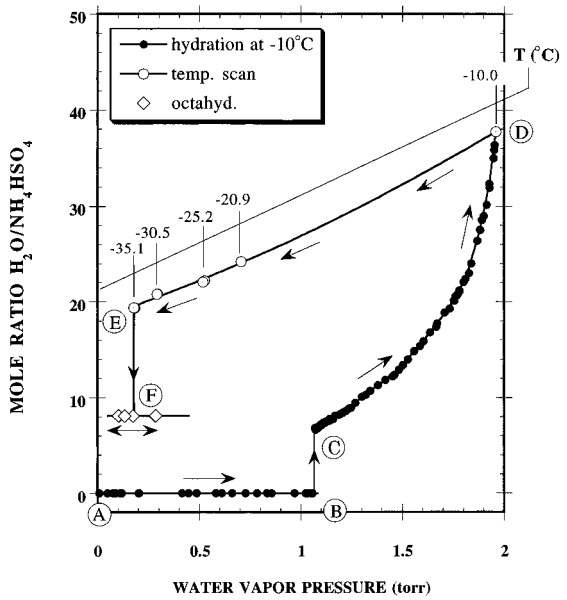

Figure 3. Plot of particle mass expressed in mole ratio H_2O/NH_4HSO_4 vs water vapor pressure in Torr illustrates a hybrid cycle in which the first step of hydration was carried out at constant temperature of −10 °C (A−D), and in the second step the water vapor was regulated to be equal to that of ice and the temperature was lowered (D−F). At −10 °C the anhydrous phase deliquesced at 1.08 Torr (B−C). Increasing the water vapor pressure from point C forward produces a more dilute solution droplet up to point D where the water vapor pressure is equal to that of ice. At this point the chamber was sealed and the temperature was lowered. This procedure guaranteed that the water vapor pressure follows the ice vapor pressure along the cooling path from −10 °C to (D−F). Along this path of decreasing water vapor pressure and decreasing temperature the solution droplets spontaneously transforms to the octahydrate phase at −35.1 °C (E−F).

solution at −31.5 °C. On the reverse cycle (F−G) the efflorescence transition (G) occurs at a RH that is lower than the anhydrous to octahydrate transition, and consequently the octahydrate phase does not form along this dehydration path.

To complete the section of the phase diagram in which ice is the stable precipitate, we performed the experiment in the temperature scanning mode. Figure 3 illustrates this procedure. First, the particles were deliquesced at −10 °C (path A−B−C), and the water vapor pressure was increased to the point where it became constant, indicating that it is in equilibrium with the ice vapor pressure at this temperature (path C−D). The chamber was then sealed and the temperature decreased, as illustrated by path D−E−F. This procedure assured that, along the D−E−F path, the water vapor pressure was maintained equal to that of ice. The particle composition along the D−E path as a function of temperature is that of an NH_4HSO_4 solution at equilibrium with ice. Note that, along this path of decreasing RH, efflorescence occurs (transition E−F at −35.1 °C) to form $NH_4HSO_4 \cdot 8H_2O$.

Discussion

Equilibrium Phase Diagram. Data such as those shown in Figures 1−3 were used to construct the NH_4HSO_4/H_2O phase diagram. Figure 4 shows the NH_4HSO_4/H_2O equilibrium phase diagram in the composition−temperature domain. The pure solution region is designated by the striped area and the three solid phases: ice, anhydrous NH_4HSO_4, and octahydrate are labeled. Two eutectic points at −33.5, and −30 °C for the octahydrate−ice and the anhydrous−octahydrate phases, respectively, were determined. The narrow stability range for the octahydrate phase may explain why it has thus far escaped

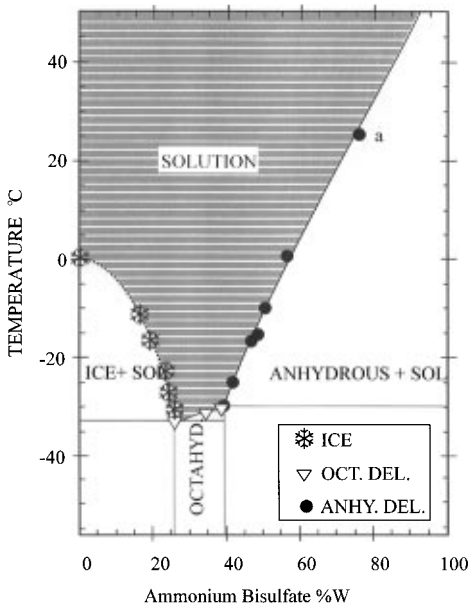

Figure 4. Equilibrium phase diagram for ammonium bisulfate and water in a temperature vs composition plot, showing the three solid phases: ice, octahydrate, and anhydrous. The dotted line in the ice + solution region is based on the data presented in Figure 3. The solid circles are based on the observed deliquescence transitions of the anhydrous phase, and the triangles represent the observed deliquescence transitions of the octahydrate phase. The points marked "a" is from Tang et al.[8]

detection. The only data point that was available prior to the present work labeled **a** in Figure 4 is from Tang et al.[8]

Since atmospheric conditions are specified in terms of temperature and RH, from the perspective of understanding atmospheric processes, phase diagrams presented in the water vapor pressure−temperature domain are much more useful. Figure 5A shows the observed equilibrium phase transition in this system in a $\log(p_w)$ vs $1/T$ plot; Figure 5B is an expanded view of the low temperatures. As in Figure 4, the striped area designates the pure solution region and the deliquescence transition lines are marked by a thick solid line. The solid−solid anhydrous to octahydrate phase transition line is indicated by clear squares. For reference, the water−ice frost line and the liquid water vapor pressure are also shown.

In the expanded view (Figure 5B) all four phases can be found. The shaded area marks the range of conditions where the octahydrate is the equilibrium phase. The rest of the symbols are as indicated in Figure 5A.

In the $\log(p_w)$ vs $1/T$ plot the deliquescence points of the anhydrous NH_4HSO_4 (solid circles) form a nearly straight line. As shown in Figure 6 in a plot of RH vs temperature, the deliquescence transitions in this system exhibit a strong dependence on temperature, from 40% RH at 25 °C to 70% RH at −33.5 °C.

We have previously reported on the unique nonequilibrium crystalline phases that form in all of the bisulfate aerosol systems. The single particle room temperature experiments[9] have shown that in NH_4HSO_4 the equilibrium and the metastable phase form with equal probability. These two distinct crystalline anhydrous NH_4HSO_4 forms have different deliquescence points at 37% RH and 40% RH. Of the two, the second was shown to be the room temperature equilibrium phase. The fact that all the observed deliquescence points in the present experiments, conducted at lower temperatures, fall on a single line indicates that only one of these forms is accessible at low temperatures. To determine which of the two phases is the low-temperature form, a linear fit to the low-temperature data alone was

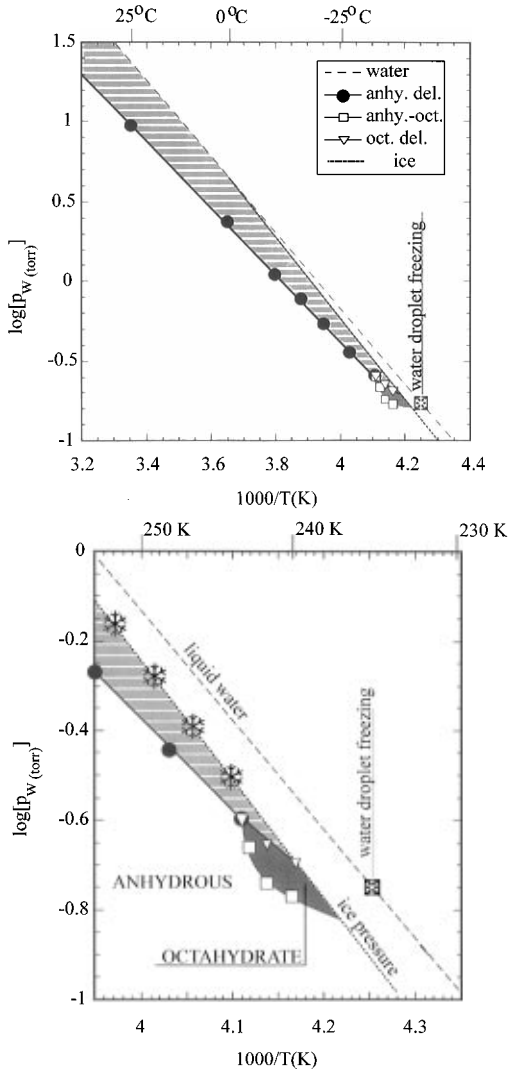

Figure 5. (A, top) Plot of the ammonium bisulfate−water equilibrium phase diagram in the $\log(p_w)$ vs $1/T$ domain. The deliquescence points of the anhydrous (solid circles) form a straight line. The deliquescence points of the octahydrate phase are shown as triangles. The anhydrous to the octahydrate phase transitions are marked by the open squares. The figure shows the water−ice frost line as well as the liquid water vapor pressure as a function of temperature. The pure water droplet freezing point is also marked. (B, bottom) An expanded view of the low-temperature region of (A).

extrapolated to 25 °C, yielding a deliquescence point of 40.5 ± −0.5% RH, consistent with the equilibrium phase.

Metastability Phase Diagram. In hygroscopic aerosols a useful rule of thumb is that phase transformations along the path of increasing RH occur at equilibrium, while phase transformations encountered along the reverse path commence from a metastable state.[9] To characterize the metastable transformations, we need a different type of (nonequilibrium) phase diagram, the boundaries of which define the boundaries of the metastable state(s). We can think of this as a "metastability phase diagram" whose boundaries mark the fundamental limit to metastability due to homogeneous nucleation. For example, measurements of the temperature at which homogeneous nucleation of supercooled liquid water occurs as a function of external pressure between 0 and 3 kbar[10] define the metastable phase boundary for pure supercooled water and provide a very valuable reference for understanding the single component nucleation mechanism. In this paper we have examined the effects of composition on homogeneous nucleation as a function of temperature.

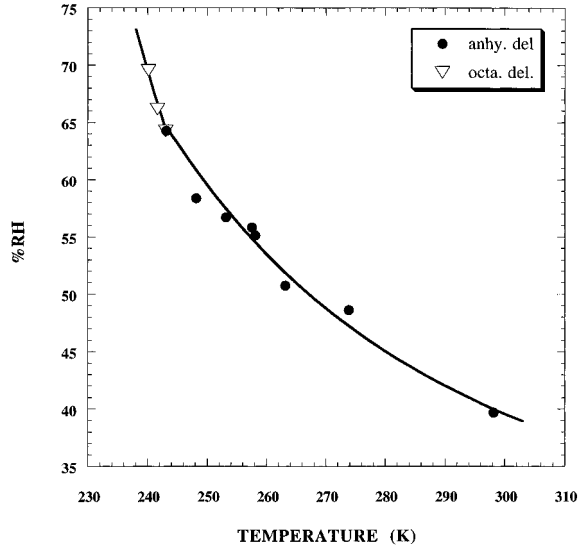

Figure 6. Plot of the deliquescence transitions in % RH for ammonium bisulfate as a function of temperature.

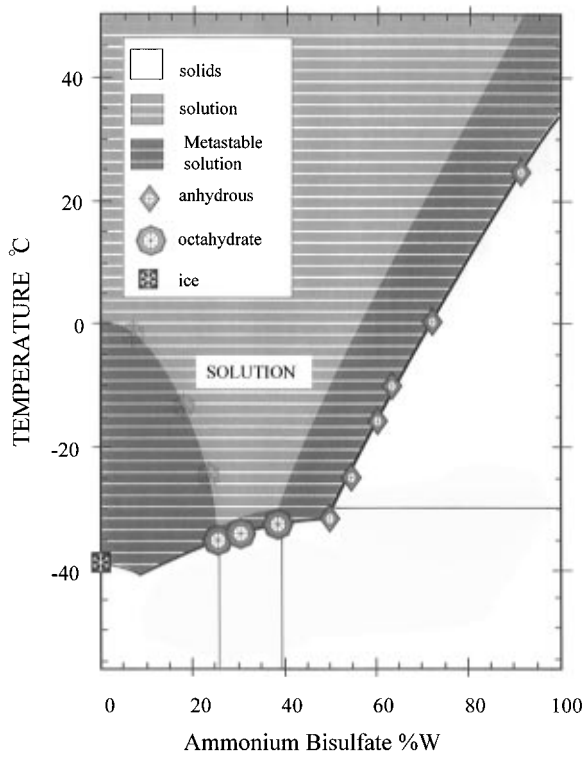

Figure 7. Metastability phase diagram for ammonium bisulfate and water in a temperature vs composition plot. The region of metastable solution droplet is indicated by the dark striped gray area, and for reference the equilibrium solution droplets are designated as in Figure 4. The efflorescence transitions forming either anhydrous or the octahydrate phases are labeled. The freezing point of pure water droplets is also shown.

Boundaries in equilibrium phase diagrams indicate the conditions of coexistence of two (or more) phases, and by analogy, boundaries in the metastability phase diagram indicate the conditions of coexistence (unstable equilibria) of the metastable phase with the critical nucleus (or nuclei) under conditions that the nucleation threshold is reached (rates of nucleation near unity). The metastability phase diagram represents a map of conditions where metastable to stable phase transformations occur, as such it is expected to be somewhat dependent on particle size. It is thus somewhat remarkable that distinct and reproducible boundaries to metastability are

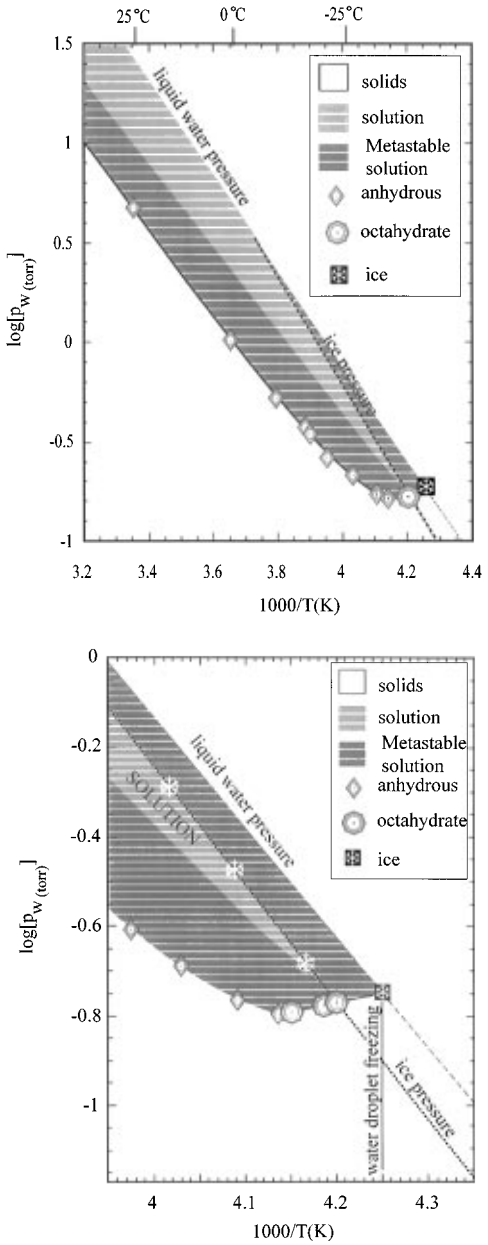

Figure 8. (A, top) Plot of the ammonium bisulfate−water metastability phase diagram in the $\log(p_w)$ vs $1/T$ domain. The efflorescence points of supersaturated solution droplets to the two different crystalline phases of this binary system are labeled. Note that the efflorescence transitions form a well-defined continuos line. (B, bottom) An expanded view of the low-temperature region in (A).

observed—given that the nucleation rate is controlled by kinetic as well as thermodynamic conditions. Nevertheless, observed homogeneous nucleation conditions are reproducible and appear to fall on continuous, well-defined boundaries. Roughly we understand that this behavior results because the rate of nucleation (in theory) has a characteristic exponential-prefactor structure with the thermodynamics in the exponent, which greatly dominates the nucleation rate.

A second important distinction is that equilibrium is a thermodynamic condition that applies between two or more *extended* phases, while the metastability equilibrium is between an extended supercooled phase and a *nanoscale* critical nucleus. Thus, surface free energy, which plays no role in the equilibrium phase diagram, is of vital importance to defining the boundaries of the metastable phase.

From the experimental standpoint, much of what we know about such transitions from the metastable phase is derived from

experiments on bulk samples in contact with container walls. Under these conditions nucleation is most often initiated by a heterogeneous process involving either surface or interior impurity sites whose presence is generally random and not easily subject to experimental control. Impurity-induced nucleation occurs under different levels of supercooling for the simple reason that different impurity sites have different abilities to initiate the process. In contrast, both theory and experiments on ultrapure phase samples show very well-defined phase transition points. The freezing of pure water droplets, for example, shows that the nucleation rate changes 4 orders of magnitude over a span of 2 °C.[11]

In a recent study of the freezing of sulfuric acid droplets, it was found that the observed freezing points form a line in the temperature−composition domain not unlike the equilibrium ice/solution coexistence line, except that it is shifted by some 40 °C.[12] This behavior is not limited to ice formation. We have recently investigated a variety of hygroscopic salts, all of which show that efflorescence occurs along well-defined lines.[13,14]

The metastability phase diagram for NH_4HSO_4 is constructed by combining our experimentally observed efflorescence points such as E and G in Figures 1 and 2, respectively, or E in Figure 3. The resultant phase diagram is presented in Figures 7 and 8 in the temperature/composition and water−pressure/temperature domains, respectively. We have observed three distinct types of metastable to stable transformations in this system. Upon efflorescence the supersaturated solution droplets can transform to either the anhydrous or the octahydrate phases. At all temperatures above −32.5 °C, the anhydrous phase forms, while below −32.5 °C the efflorescence process produced only the octahydrate phase. Metastability in this system is not limited to the solution phase. The equilibrium region where the octahydrate phase is stable is extremely limited, but once formed, this phase remains stable even at 0 RH, as long as the temperature remains below −27 °C (as observed for over 24 h). At temperatures below −38 °C—the freezing point of pure water droplets—and high RH, ice is the expected solid phase.

Conclusion

We have for the first time derived the phase diagram for the NH_4HSO_4/H_2O system and observed a new, low-temperature crystalline phase composed of NH_4HSO_4 with eight water molecules. The temperature dependence of the phase transitions either solid−solid or solid−liquid have been mapped, and the metastable, supersaturated solution efflorescence conditions have also been identified.

The phase diagrams presented in Figures 4, 5, 7, and 8 can now be used to predict the phase and composition of an NH_4HSO_4 aerosol under any atmospheric condition, provided the history of the air parcel is known. An anhydrous particle will not deliquesce as long as its temperature is kept below −33.5 °C. It can, however, increase in size (roughly double its mass) as its RH is increased due to the absorption of water and transform from the anhydrous to the octahydrate phase. At temperatures between −30 and −33.5 °C an increase in RH would first induce a transition from the anhydrous to the octahydrate state and eventually lead to deliquescence. Metastable solution droplets can be found at temperatures lower than −33.5 °C, but only if initially formed at a higher temperature.

Acknowledgment. This research was performed under the auspices of the U.S. Department of Energy under Contract DE-AS02-76H00016. We also thank Brookhaven National Laboratory for the LDRD support.

References and Notes

(1) Charlson, R. J.; Schwartz, S. E.; Hales, J. M.; Cess, R. D.; Coakely, J. A.; Hansen, J. E. *Science* **1992**, *255*, 423.
(2) Twomey, S. In *Atmospheric Aerosols;* Elsevier Scientific Publishing: Dordrecht, 1977.
(3) Tang, I. N.; Munkelwitz, H. R. *J. Colloid Interface Sci.* **1989,** *128*, 289.
(4) Tang, I. N.; Munkelwitz, H. R. *Atmos. Environ.* **1993**, *27A*, 467.
(5) Tabata, *S. J. Appl. Meteorol.* **1973**, *12*, 1410.
(6) Tang, I. N.; Munkelwitz, H. R. *J. Geophys. Res.* **1994**, *99*, 18801.
(7) Tang, I. N.; Munkelwitz, H. R. *J. Aerosol Sci.* **1977**, *8*, 321.
(8) Tang, I. N.; Munkelwitz, H. R.; Davis, J. G. *J. Aerosol Sci.* **1978**, *9*, 505.
(9) Tang, I. N.; Fung, K. H.; Imre, D. G.; Munkelwitz, H. R. *Aerosols Sci. Technol.* **1995**, *23*, 443.
(10) Kanno, H.; Speedy, R. J.; Angell, C. A. *Science* **1973**, *189*, 880.
(11) Kraemer ,B.; Schwell, M.; Hueber, O.; Voritisch, H.; Leisner, T.; Ruel, R.; Baumgaertel, H.; Voeste, L. *Ber. Bunsen-Ges. Phys. Chem.* **1996**, *11*, 1911.
(12) Bertram, A. K.; Patterson, D. D.; and Sloan, J. J. *J. Phys. Chem.* **1996,** *100*, 2376.
(13) Tang, I. N. In *Generation of Arosols;* Willeke, K., Ed.; Ann Arbor Science: Ann Arbor, MI, 1980.
(14) Imre, D. G.; Xu, J. To be published.